

${}^4\text{He}(\vec{n},n){}^4\text{He}$ analyzing power in the energy range from 15 to 50 MeV

H. Krupp, J. C. Hiebert,* H. O. Klages, P. Doll, J. Hansmeyer, P. Plischke, and J. Wilczynski
Kernforschungszentrum Karlsruhe, Institut für Kernphysik 1, D-7500 Karlsruhe, Federal Republic of Germany

H. Zankel

Institut für Theoretische Physik, Universität Graz, 8010 Graz, Austria

(Received 10 April 1984)

Angular distributions of the analyzing power $A_y(\theta)$ for the elastic n - ${}^4\text{He}$ scattering have been measured in the energy range 15–50 MeV. A continuous energy polarized neutron beam was produced using a 52 MeV polarized deuteron beam incident on a liquid deuterium target. A liquid helium scintillation detector was used as a scattering sample. Scattered neutrons were detected with 14 scintillation detectors. Multiparameter data acquisition was performed to discriminate against background events. The incident neutron energy was determined off line by cuts in the incident time-of-flight spectra. The data were normalized in the backward angle maxima by previous N - ${}^4\text{He}$ data. The results were used as input in a series of phase shift analyses. Coulomb correction procedures to p - ${}^4\text{He}$ phase shifts have been used to provide n - ${}^4\text{He}$ predictions. The validity of these procedures has been tested. A set of n - ${}^4\text{He}$ phase shifts, varying smoothly with energy, is given which reproduces the new data very well.

I. INTRODUCTION

The elastic scattering of neutrons from ${}^4\text{He}$ nuclei has been the subject of numerous studies during the past two decades. This process, together with the charge-symmetric p - ${}^4\text{He}$ elastic scattering, has been of special interest because it is the simplest scattering process giving information on the spin-dependent part of the nuclear interaction, and significant progress has already been made in the description of N - ${}^4\text{He}$ scattering in terms of the fundamental nucleon-nucleon (N-N) interaction. Experimentally, ${}^4\text{He}$ has been used extensively as a polarization analyzer in nucleon polarization measurements, and accurate N - ${}^4\text{He}$ phase shifts are necessary for these applications. In the past, the determination of n - ${}^4\text{He}$ phase shifts has relied heavily on the more numerous and more precise p - ${}^4\text{He}$ scattering data. With improved n - ${}^4\text{He}$ data it is hoped that the charge symmetry of the nuclear force can be tested if Coulomb effects are handled appropriately.

At energies above 15 MeV the precision of the n - ${}^4\text{He}$ analyzing power data is generally not adequate to perform a quantitative comparison with p - ${}^4\text{He}$ data. The only qualitative comparisons in the literature have been made by Lisowski *et al.*¹ at $E_n=20.9$ MeV and by York *et al.*² at $E_n=50.4$ MeV. Accuracy for neutron data must approach the standard of the proton data to permit meaningful comparison with Coulomb corrected p - ${}^4\text{He}$ analyzing power data.

This paper reports on measurements of n - ${}^4\text{He}$ asymmetries, $\epsilon(\theta)$, for ten neutron energies in the range 15–50 MeV. These asymmetries are converted to analyzing powers by normalizing the large backward angle maximum to (i) existing n - ${}^4\text{He}$ phase shift calculations of $A_y(\theta)$ below 20 MeV, (ii) p - ${}^4\text{He}$ $A_y(\theta)$ measurements between 25 and 30 MeV, and (iii) n - ${}^4\text{He}$ predictions based on Coulomb corrected p - ${}^4\text{He}$ phase shifts above 30 MeV.

Our new values of $A_y(\theta)$ for the n - ${}^4\text{He}$ scattering are compared to previous data sets and, at 17, 40, and 50 MeV to predictions obtained by applying Coulomb corrections, including approximate contributions from Coulomb distortions, to p - ${}^4\text{He}$ phase shifts.

The polarized neutrons were obtained in the ${}^2\text{H}(\vec{d},\vec{n})X$ reactions at 0° with a vector polarized deuteron beam at 50 MeV. Having converted the measured asymmetries to analyzing powers, the neutron polarization, $P_n(E_n)$, and finally the spin transfer coefficient, $K_y^{\prime\prime}(E_n)$, for the ${}^2\text{H}(\vec{d},\vec{n})X$ reactions at 0° and $E_d=50$ MeV was determined at the ten neutron energies. A set of smoothly varying n - ${}^4\text{He}$ phase shifts is presented covering the 15–50 MeV region.

II. EXPERIMENT

A. Apparatus and measurement

The experiment was carried out at the polarized neutron facility POLKA at the Karlsruhe cyclotron, shown in Fig. 1. The apparatus has been described in detail elsewhere,³ so only a brief description is given here.

Polarized deuterons are produced by a Lamb-shift-type ion source and bunched to a frequency of 11 MHz before acceleration to an energy of 52 MeV. The polarization of the deuteron beam is measured and continuously monitored by use of the elastic \vec{d} - ${}^{12}\text{C}$ scattering at $\theta_{\text{lab}}=\pm 47^\circ$ in a beam-line polarimeter. The deuteron spin is reversed at the ion source every 100 sec. The deuterons passing through the polarimeter impinge on a liquid deuterium target with $12\ \mu$ thick molybdenum foils as entrance and exit windows. The target thickness used was 1 cm, corresponding to an energy loss of ~ 4 MeV. After the target, the deuterons are bent by 60° and stopped in a shielded beam dump. The target is surrounded by massive shield-

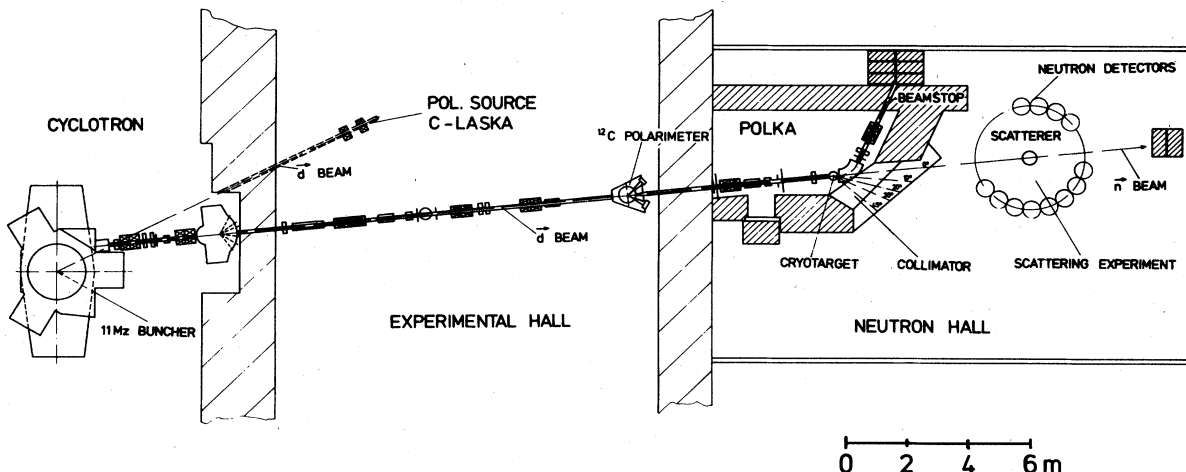


FIG. 1. Schematic view of the polarized neutron facility POLKA at the Karlsruhe cyclotron. The neutron beam is used outside the shielded target area for scattering experiments. The distance from the cryotarget to the scattering sample is 6 m.

ing. A special iron-polyethylene collimator at forward angles allows the extraction of narrow neutron beams at five different angles. In the present experiment the 0° collimator tube was used. The neutrons produced in the ${}^2\text{H}(\bar{d}, \bar{n}){}^3\text{He}$ reaction and in ${}^2\text{H}(\bar{d}, \bar{n})X$ breakup processes are collimated to form a beam with a cone of about 8×10^{-5} sr.

The scattering experiment is performed at a distance of 6 m from the production target, where the beam is about 60 mm wide. Here the neutrons interact with a liquid- ${}^4\text{He}$ scintillating sample^{4,5} which is 70 mm in diameter and 75 mm high. The use of a similar liquid-helium sample has been described in great detail in Ref. 2. The scattered neutrons are detected at 1 m by 14 neutron detectors, upright cylinders filled with NE213, which are 140 mm in diameter and 200 mm high. At four laboratory angles (100° , 110° , 120° , and 130°) symmetric pairs of detectors were used. The scattering plane lies 2.5 m above floor level to reduce neutron backscattering from the concrete.

Data acquisition was performed event by event using a ND4420 multichannel analyzer system (Nuclear Data). First, the incident neutron energy is determined by measuring the time of flight to the ${}^4\text{He}$ sample; second, the recoil pulse height in the ${}^4\text{He}$ sample and the time of flight of the scattered neutron to the side detector determine the kinematics of the elastic scattering; and third, pulse-height and pulse-shape information from the neutron detectors is used to discriminate against γ -ray events and to apply thresholds off line. In addition, a signal which contains the detector number and the spin up/down information on the deuteron beam is generated and stored on tape. Data were taken in 2 h "runs" for a total of about 250 h.

B. Data reduction

In the off-line analysis the data were corrected run by run for instabilities, e.g., for time shifts in the incident TOF spectra and for small gain changes in the scintillator

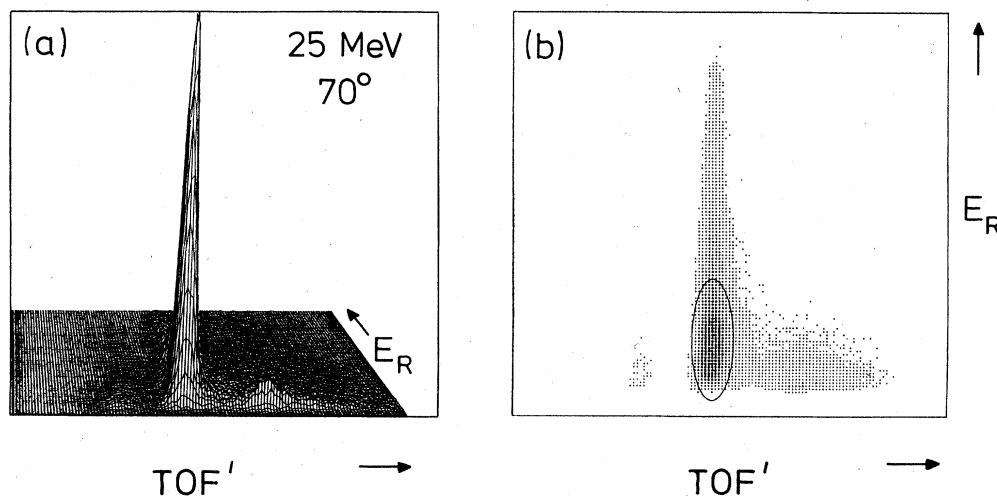


FIG. 2. Two-dimensional representation of the \bar{n} - ${}^4\text{He}$ scattering data at 25 MeV and $\theta_{\text{lab}} = 70^\circ$. The isometric display (a) shows the relative importance of elastic scattering events and background from inelastic processes and multiple scattering. In the contour plot (b) the solid line indicates the region of integration in the data analysis (see the text).

signals. After applying all necessary corrections the data were split up according to the 14 neutron detectors. In the next step n - γ discrimination was performed and a lower pulse height threshold was set. The 14 data sets were subdivided into 10 incident-energy bins by appropriate cuts in the incident TOF spectra, and the separation in spin up/down was performed. Finally, the data were represented by 280 two-dimensional matrices. Figure 2 shows the data for $E_n = 25$ MeV and $\theta_{\text{lab}} = 70^\circ$. It can be seen that uncorrelated background is small. The region of the elastic scattering peak is clearly separated from all backgrounds but multiple scattering. From the events integrated in the elastic peak the spin-dependent asymmetry $\epsilon(E_n, \theta)$ was calculated. This was done for the symmetric pairs of detectors using the relation

$$\epsilon = \frac{(L \uparrow R \downarrow)^{1/2} - (L \downarrow R \uparrow)^{1/2}}{(L \uparrow R \downarrow)^{1/2} + (L \downarrow R \uparrow)^{1/2}}$$

by which experimental asymmetries are canceled in first order. From the same data the spin up/down flux ratio R was determined using $R = (L \uparrow R \uparrow / L \downarrow R \downarrow)^{1/2}$. In the present experiment this ratio was $R = 0.985$. For the angles measured by one detector only, the "spin down" count rates were multiplied by R before calculating the asymmetry

$$\epsilon = \frac{N \uparrow - N \downarrow}{N \uparrow + N \downarrow}$$

In this way angular distributions of the measured asymmetries were obtained for ten energy bins, centered at 15, 17, 19, 25, 27.5, 30, 33, 36, 40, and 50 MeV.

These asymmetries had to be corrected for finite geometry effects and for multiple scattering of the neutrons in the helium sample. The code PMS (Ref. 6) has

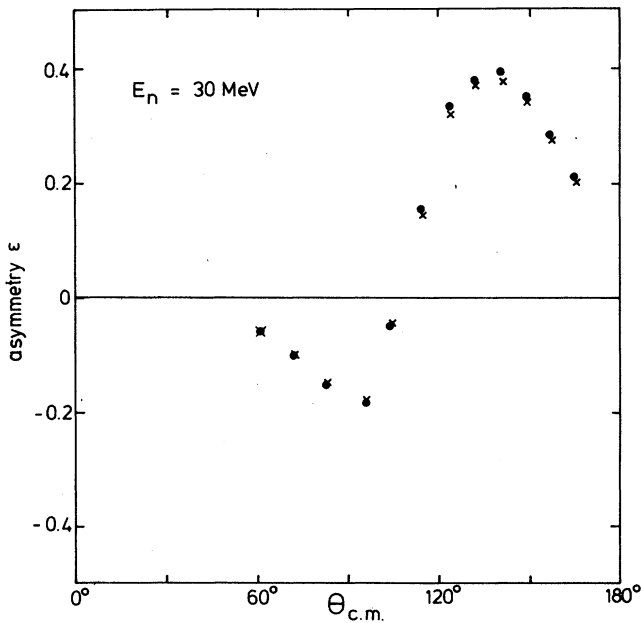


FIG. 3. Measured asymmetries (crosses) for the \bar{n} - ^4He scattering at 30 MeV and final values of ϵ (dots) corrected for multiple scattering and finite geometry effects.

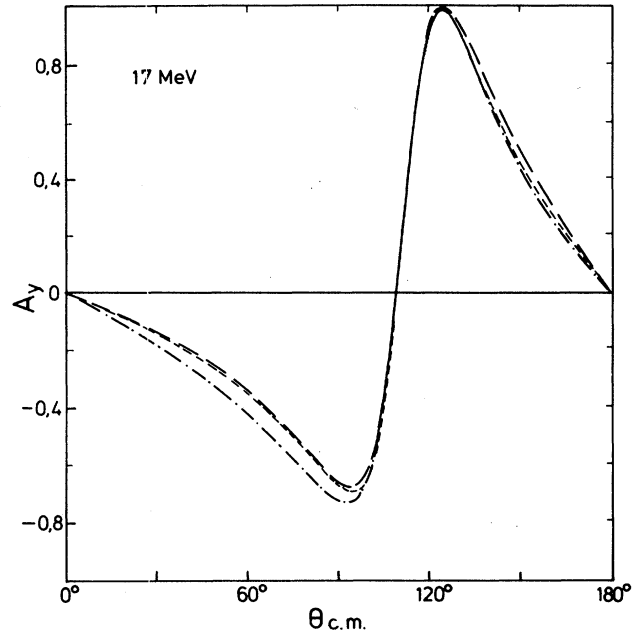


FIG. 4. \bar{n} - ^4He analyzing power predictions at 17 MeV: (a) dashed-dotted line: R -matrix calculation (Ref. 8); (b) long-dashed line: n - ^4He phase shifts (Ref. 14); and (c) dashed line: Coulomb corrections applied to p - ^4He shifts from Ref. 21.

been modified and was used for this purpose. From energy dependent n - ^4He phase shifts as input, the point-geometry differential cross section and analyzing power is calculated for each scattering in the helium. The probability is calculated for multiple scattering and the change in asymmetry due to multiple scattering and to finite geometry is determined. In Fig. 3 the measured and corrected asymmetries for the 30 MeV distribution are shown. In general, the correction factors obtained are rather small, e.g., they decrease from 1.12 at 15 MeV to 1.03 at 50 MeV for the backward angle maximum, whereas in the region around 100° these factors vary between 1.05 and 1.09, nearly independent of energy.

C. Normalization procedure

The asymmetries are, normally, converted to analyzing powers taking

$$A_y(E_n, \theta) = \epsilon(E_n, \theta) / P_n(E_n)$$

In the present case the polarization in the neutron beam as a function of energy was not known *a priori*. In the recent work of York,⁷ however, using the $^2\text{H}(\vec{d}, \vec{n})$ reaction at 50.4 MeV, it was shown that the 0° neutron beam was highly polarized, both in the $^2\text{H}(\vec{d}, \vec{n})^3\text{He}$ two-body reaction peak and in the high energy part of the deuteron breakup distribution. Another conclusion of this work was that the backward angle maxima of the analyzing power distributions for the \bar{p} - ^4He and the \bar{n} - ^4He channels are equal within the experimental errors. Our calculations revealed that Coulomb effects are very small in this angular region, even in the energy range below 20 MeV (see Fig. 4), and that different approaches for Coulomb correc-

TABLE I. Neutron beam polarization and deduced ${}^2\text{H}(\vec{d},\vec{n})$ spin transfer coefficients $K_y^y(0^\circ)$ as a function of neutron energy.

E_n (MeV)	\bar{E}_n (MeV)	P_n (%)	K_y^y
15±1.0	15.00	20.6±0.5	0.267±0.007
17±1.0	17.03	25.2±0.5	0.326±0.007
19±1.5	19.08	31.9±1.0	0.413±0.012
25±1.5	25.00	44.6±1.3	0.578±0.017
27.5±1.0	27.44	46.1±1.4	0.597±0.018
30±1.5	29.85	46.9±1.4	0.608±0.018
33±1.5	32.85	47.1±1.4	0.610±0.018
36±2.0	35.80	46.8±1.4	0.606±0.018
40±2.0	39.72	47.5±1.4	0.615±0.018
50±2.0	50.00	46.7±1.6	0.605±0.021

tions lead to consistent predictions. Details will be given in Sec. III.

We normalized the data using three different methods: (i) At 15 and 17 MeV we took backward angle predictions from n - ${}^4\text{He}$ phase shifts of Bond and Firk;⁸ (ii) at 19, 25, 27.5, and 30 MeV we used p - ${}^4\text{He}$ data of Bacher *et al.*⁹ at slightly shifted energies according to the energy shift of the $\frac{3}{2}^+$ resonance in the $A=5$ systems (we had to interpolate the data of Ref. 9 for this purpose); (iii) For the energy range 33–40 MeV we got n - ${}^4\text{He}$ predictions by applying Coulomb corrections to the p - ${}^4\text{He}$ phase shifts of Houdayer *et al.*¹⁰ and, at 50 MeV, to the solution II of Saito.¹¹

D. Neutron beam polarization

With the above-mentioned normalizations, the polarization of the neutron beam $P_n(E_n)$ has been determined with an absolute scale error of 2–4%. The results are listed in Table I together with the width and average energy for each bin. It should be noted that the values for P_n depend linearly on the polarization of the deuteron beam. Taking the value of $A_y=0.360$ for the \vec{d} - ${}^{12}\text{C}$ scattering at 52 MeV from Ref. 12, we get $P_d=0.515$ for the measured deuteron asymmetry $\epsilon=0.278$.

The energy dependence of the spin transfer coefficient $K_y^y(0^\circ)$ in the breakup part of the spectrum is in good agreement with the less accurate data of York⁷ and with a simple stripping model,¹³ assuming there is no spin flip in the breakup processes and a deuteron D -state probability of 4%.

The first result of this experiment is that the polarized neutron beam from POLKA is useful for scattering experiments in the energy range from 15 to 50 MeV simultaneously.

The new A_y data for the n - ${}^4\text{He}$ scattering will be compared to previous results and discussed in more detail in Sec. IV.

III. COULOMB CORRECTIONS IN n - ${}^4\text{He}$ SCATTERING

Predicted values for n - ${}^4\text{He}$ observables can be obtained by calculating Coulomb corrections to p - ${}^4\text{He}$ phase shifts. These Coulomb-corrected calculations have been used in the present analysis as follows:

- (1) to normalize the polarization of the neutron beam for energies above 30 MeV, i.e., calculate n - ${}^4\text{He}$ analyzing powers in the backward angle maximum;
- (2) to generate pseudodata on differential cross sections for n - ${}^4\text{He}$ scattering above 30 MeV in order to make possible a phase-shift analysis of the present data; and
- (3) for the interpretation of a direct comparison of measured n - ${}^4\text{He}$ and p - ${}^4\text{He}$ analyzing powers.

The exact calculation of these Coulomb contributions can only be performed in a model dependent manner. Therefore, approximate calculations have been attempted, especially in the case of the more complex few-body systems. At the simplest level pure Coulomb phase shifts are added appropriately to yield a “Coulomb modified” scattering amplitude. For N - ${}^4\text{He}$ scattering Hoop and Barschall¹⁴ supplemented this “zero-order” Coulomb approximation by an energy shift which is motivated by the energy difference of the excited states in ${}^5\text{Li}$ and ${}^5\text{He}$ near inelastic threshold. At a higher level of sophistication the Coulomb distortion has been treated within R -matrix theory¹⁵ for energies below inelastic threshold. Another approximation expresses the Coulomb modifications to the nuclear transition matrix within the context of integral equations. This method was developed initially for N - N scattering,¹⁶ yielding an on-shell expression for the Coulomb corrections. Later on, a similar simple on-shell formula¹⁷ was derived from the Faddeev equations where the Coulomb distortion to N - d scattering is described in an effective two-body manner and the extended charge distribution of the scattering particles is accounted for. This approach has been successfully extended to other few-body systems.^{18,19} It is particularly well suited to the N - ${}^4\text{He}$ scattering system since an effective two-body treatment is a realistic assumption for proton scattering from the tightly bound helium nucleus. The effectiveness of this approach has already been demonstrated below 20 MeV (Ref. 19) where good agreement was found with the results from R -matrix calculations. It is worth noting that a similarity exists between the two approaches, e.g., the on-shell expansion in the Coulomb distorted transition amplitude is related to the matching of the Coulomb wave function at the surface.

The on-shell approximation to the five-body reaction matrix reads for each total angular momentum

TABLE II. \bar{n} - ^4He analyzing powers and (absolute) errors, both in percent.

E_n (MeV)	15		17		19		25		27.5	
$\theta_{\text{c.m.}}$	A_y	ΔA_y	A_y	ΔA_y	A_y	ΔA_y	A_y	ΔA_y	A_y	ΔA_y
61.4°	-42.6	2.1	-41.3	1.1	-38.5	0.5	-19.3	0.3	-15.8	0.5
72.4°	-56.6	2.2	-48.5	1.1	-48.4	0.6	-30.2	0.4	-24.9	0.6
83.5°	-68.8	1.9	-70.4	1.1	-60.2	0.6	-44.9	0.4	-36.4	0.5
96.4°	-85.0	2.8	-81.4	1.8	-68.1	0.9	-59.0	0.5	-41.8	0.8
104.8°	-57.9	4.3	-57.1	2.6	-38.6	1.3	-14.4	0.6	-4.8	0.8
114.9°	42.0	2.5	49.9	1.5	48.9	0.7	50.6	0.3	52.3	0.5
124.3°	99.2	1.8	98.8	1.1	94.0	0.6	83.4	0.2	78.1	0.3
123.8°	92.6	1.6	92.9	1.0	79.8	0.5	82.6	0.2	82.2	0.2
141.5°	69.9	1.5	71.1	1.0	59.1	0.5	70.7	0.2	75.7	0.9
149.9°	54.2	2.5	49.6	1.4	41.6	0.8	57.4	0.5	68.4	0.8
157.8°	37.9	3.3	36.7	2.1	30.6	1.1	42.1	0.7	56.5	1.1
165.7°	24.6	3.3	26.9	1.9	19.7	1.0	30.3	0.7	40.0	1.1

$$Q_l^{\text{sc}}(q) = Q_l^s(q) + \frac{2\mu e^2}{\pi q \tilde{C}_l(q)} \left| Q_l^s(q) + q \frac{d}{dq} Q_l^s \right| - \frac{\pi}{2} \tilde{V}_l(q),$$

where $\tilde{C}_l(q)$ and $\tilde{V}_l(q)$ are terms involving the Coulomb potential and the electric form factors of the proton and the ^4He nucleus, respectively. Here q is the on-shell c.m. momentum and μ is the reduced mass of the system. To

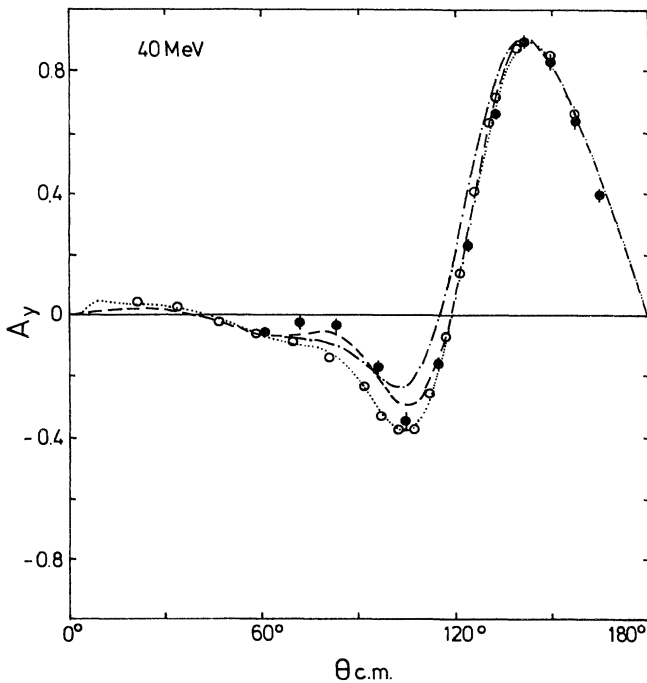


FIG. 5. N - ^4He analyzing power at 40 MeV: full circles, this work, n - ^4He ; open circles, Ref. 8, p - ^4He ; dotted line, p - ^4He phase-shift analysis of Ref. 24; dashed-dotted line, first-order Coulomb corrections applied; and dashed line, n - ^4He prediction from second-order Coulomb corrections (see the text).

utilize this formula for calculating charge symmetric n - ^4He predictions on the basis of p - ^4He data it is solved by an iterative inversion. As input the on-shell Coulomb modified nuclear p - ^4He reaction matrix and its momentum derivatives are required. This requirement restricts the application of the method to those cases where the on-shell amplitude varies smoothly with energy. Thus one must avoid the region of the inelastic threshold or try, as a further approximation, background phase shifts.¹⁹ For a wider application of these Coulomb distortion corrections in light nuclear systems a term of second order in the nuclear amplitude has to be incorporated since it contributes strongly at narrow resonances.²⁰

Below 20 MeV, energy dependent phase-shift analyses are available, and in the present work the p - ^4He results of Schwandt *et al.*²¹ have been used. Between 20 and 40 MeV a low-order polynomial fit has been obtained to the p - ^4He phase shifts of Houdayer *et al.*¹⁰ The Houdayer phase shifts match the phase shifts below 20 MeV and display a relatively smooth energy dependence (except at inelastic threshold and near 33 MeV). For energies above 40 MeV, the Houdayer phase shifts do not reproduce the analyzing power data of Imai *et al.*,²² whereas the analysis of Saito¹¹ produced good fits to the Imai data. Saito found two equivalent phase shift solutions in the 40–60 MeV region. Because the Saito II phase shifts more nearly match the Houdayer values at 40 MeV, an energy dependent fit to the Saito solution II has been used in the present work. First-order relativistic corrections to the Coulomb scattering amplitude as given by Foote *et al.*²³ have been included in calculating the p - ^4He observables.

These charge-symmetric n - ^4He predictions of $A_y(\theta)$ have been used above 30 MeV to determine the polarization of the neutrons in the POLKA beam. A search was conducted to find an angular region where the proton analyzing powers are least sensitive to Coulomb effects; where the zero-order Coulomb corrections (pure Coulomb contribution) and the Coulomb distortion corrections are small. Such behavior is indeed found in the backward angle maximum of $A_y(\theta)$ near 130° (c.m.). A comparison of

TABLE II. (Continued).

E_n (MeV)	30		33		36		40		50	
$\theta_{c.m.}$	A_y	ΔA_y	A_y	ΔA_y	A_y	ΔA_y	A_y	ΔA_y	A_y	ΔA_y
61.4°	-13.0	0.5	-10.7	0.6	-8.1	0.9	-5.5	1.5	-10.6	3.1
72.4°	-21.4	0.6	-15.5	0.9	-11.2	1.1	-2.8	2.0	2.6	2.7
83.5°	-32.5	0.6	-25.4	0.8	-16.9	1.1	-3.6	2.0	16.3	4.7
96.4°	-39.4	0.9	-37.5	1.1	-27.7	1.5	-16.4	2.5	13.0	4.4
104.8°	-10.4	0.7	-24.7	1.4	-32.9	1.8	-33.4	3.0	-25.6	6.6
114.9°	32.6	0.4	19.1	0.8	3.3	1.2	-13.5	2.0	-24.4	6.2
124.3°	70.9	0.3	59.0	0.6	42.1	0.8	23.1	1.7	-7.9	4.5
132.8°	80.2	0.3	78.8	0.4	73.1	0.5	64.4	1.0	50.8	3.0
141.5°	83.4	0.3	82.1	0.4	87.0	0.4	89.1	0.7	89.8	1.6
149.9°	74.5	0.8	78.7	1.0	79.3	1.2	84.0	2.2	88.1	4.3
157.8°	60.2	1.1	65.3	1.4	66.5	1.6	64.1	2.5	69.7	5.2
165.7°	44.7	1.1	45.5	1.4	41.7	1.6	39.1	2.4	42.5	4.9

the charge-symmetric n - ${}^4\text{He}$ prediction of $A_y(\theta)$ at 17 MeV with the results of the phase shift analysis of Hoop and Barschall¹⁴ and those from the R -matrix analysis of Bond and Firk⁸ is shown in Fig. 4. There is excellent agreement at the 125° maximum.

At 40 MeV the Coulomb corrections are essential in explaining the differences between proton⁹ and neutron analyzing powers. Applying only zero-order Coulomb corrections (simply switching off all Coulomb terms while using p - ${}^4\text{He}$ phase shifts) exaggerates the differences between the two analyzing powers. It is the Coulomb distortion that partly compensates the zero-order corrections. It can be seen in Fig. 5 that the charge symmetric n - ${}^4\text{He}$ prediction agrees very well with the measured n - ${}^4\text{He}$ analyzing powers throughout the backward peak and that the p - ${}^4\text{He}$ results are also nearly identical to the n - ${}^4\text{He}$ results throughout the peak.

Another example of the effectiveness of the on-shell approximation is given in Sec. V, where predicted cross sections are used as input in a n - ${}^4\text{He}$ phase shift analysis.

IV. RESULTS

Numerical values for the n - ${}^4\text{He}$ analyzing power determined by the described asymmetry measurements and normalizations are listed in Table II. The quoted errors include statistical uncertainties as well as spin up/down monitor errors and the uncertainties of the corrections for multiple scattering and finite geometry. Scale errors for the normalization are not included. These can be deduced from the neutron polarization uncertainties listed in Table I. In general, these errors are 2–4%.

In the energy range below 20 MeV, our data can be compared to accurate data and reliable phase shifts from numerous previous works. Even at these energies the existing data base was considerably improved. The agreement with the results of previous phase shift analyses^{14,26–29} is reasonable; the agreement with the predictions of the more recent R -matrix analysis by Bond and Firk⁸ is good. In Fig. 6 our results (full circles) at 15, 17, and 19 MeV are shown together with the data of Broste

*et al.*²⁵ (triangles) at 17.7 MeV and with the p - ${}^4\text{He}$ data of Bacher *et al.*⁹ (open circles) at 19.9 MeV. The dotted lines are the results of single energy phase shift analyses described in Sec. V; the dashed line shows the output of a Coulomb correction calculation starting from p - ${}^4\text{He}$ phase shifts of Schwandt *et al.*²¹ It can be seen that the applied method of Coulomb corrections is capable of reproducing the backward angle maximum fairly well.

In the energy range above the inelastic threshold only a very few measurements have been performed up to now. In Fig. 7 our data at 25, 27.5, and 30 MeV are plotted together with the data of Broste *et al.*²⁵ (triangles) at nearby energies. The dotted lines show the results of single energy phase shift analyses including all available data. The accuracy of the data is increased by nearly an order of magnitude, especially at 30 MeV.

Between 25 and 33 MeV the shape of the backward angle maximum is changing with energy. A similar behavior has been noted for the p - ${}^4\text{He}$ channel around 30 MeV.²⁴ There is some indication in the phase shift solutions that the P waves might be responsible for this effect. However, the change of the A_y distributions with energy is rather slow. The width of the energy bins used in the data analysis has no effect on the results within the limits of statistical accuracy. This has been checked at 25 and 50 MeV by using bins of half-width in the data analysis.

In a recent publication² York *et al.* presented n - ${}^4\text{He}$ analyzing power data and phase shifts at 50.4 MeV and a detailed comparison with the p - ${}^4\text{He}$ channel. In Fig. 8 our results at 50 MeV are shown together with the data of Ref. 2 (squares). The dotted line is the result of a new phase shift analysis including all available data. The dashed line shows the n - ${}^4\text{He}$ analyzing power prediction calculated from the "Saito II" p - ${}^4\text{He}$ phase shifts.¹¹ It should be noted that the p - ${}^4\text{He}$ analysis also includes H waves, whereas in our analysis only partial waves up to $l=4$ are taken into account. Therefore, we conclude that the slight discrepancies at the forward angles should not be emphasized.

The uncertainties of the spin transfer coefficients K_y^y

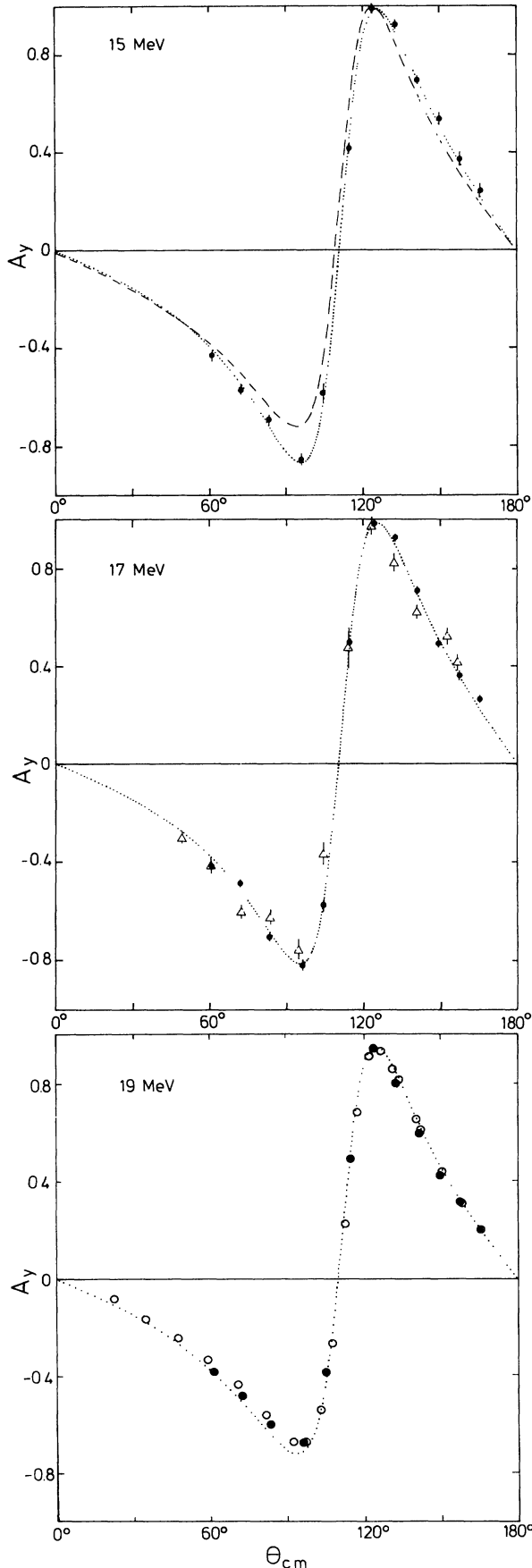


FIG. 6. \bar{n} - ${}^4\text{He}$ analyzing power at 15, 17, and 19 MeV: full circles, this work; dotted lines, phase-shift analyses (this work); dashed line, Coulomb correction prediction from p - ${}^4\text{He}$ phase shifts of Ref. 21; triangles, \bar{n} - ${}^4\text{He}$ data of Ref. 25 at 17.7 MeV; and open circles, \bar{p} - ${}^4\text{He}$ data of Ref. 9 at 19.9 MeV.

listed in Table I include both statistical and systematic errors of our determination of the neutron beam polarization. However, the error in deuteron beam polarization from the uncertainty of the ${}^{12}\text{C}(\bar{d},d){}^{12}\text{C}$ analyzing power is not included.

The value for $A_y(d-{}^{12}\text{C})$ at 52 MeV and 47° lab was determined to $A_y = 0.36 \pm 0.04$ by Mairle *et al.*¹²

V. PHASE SHIFT ANALYSIS

The parametrization of the n - ${}^4\text{He}$ scattering in terms of complex phase shifts is rather simple because of the spin- $\frac{1}{2}$ -spin-0 structure of the n - ${}^4\text{He}$ system.

We performed (single energy) phase shift analyses at the ten center energies of our data bins using in addition, all previous data in this energy range,³⁰ together with more recent differential cross section results of Drog³¹ and new precise data on total cross sections by our group,³² as well as the 50.4 MeV A_y results of Ref. 2. Starting values were taken from the phase shifts of Hoop and Barschall¹⁴ at the lower energies and from Coulomb corrected p - ${}^4\text{He}$ phase shifts above 30 MeV. Total cross sections, differential cross sections, and analyzing powers were calculated from the phase shifts and compared to the experimental data.

The code MINUIT (Ref. 33) was used to minimize the quantity χ^2 defined by

$$\chi^2 = \sum_{i,d} \left(\frac{\text{CALC}_{i,d} - N_d \text{EXP}_{i,d}}{\Delta \text{EXP}_{i,d}} \right)^2 + \sum_d \left(\frac{1 - N_d}{\Delta N_d} \right)^2,$$

where i is the individual data point index, d is the data set number, EXP is the experimental result, ΔEXP is the experimental error, CALC is the calculated result, N_d is the normalization for data set d , and ΔN is the normalization error.

It should be noted that EXP, ΔEXP , and ΔN are input data to the phase shift code, whereas the values for N_d are parameters of the minimization procedure, which starts with $N_d = 1$ for all data sets.

This method has the advantage of taking normalization errors into account, which may have been a serious problem in some of the older measurements and, even for the more recent data, are by no means negligible. On the other hand, the number of free parameters in the search procedure for the χ^2 minimum is further increased. A large number of parameters can lead to a relatively flat behavior in χ^2 if the data base is small. In the n - ${}^4\text{He}$ case that is not important below 20 MeV, but at the higher energies the problem is severe. It should be mentioned here that for most of the data sets we used in our analyses the resulting normalization deviates from unity by only a few percent.

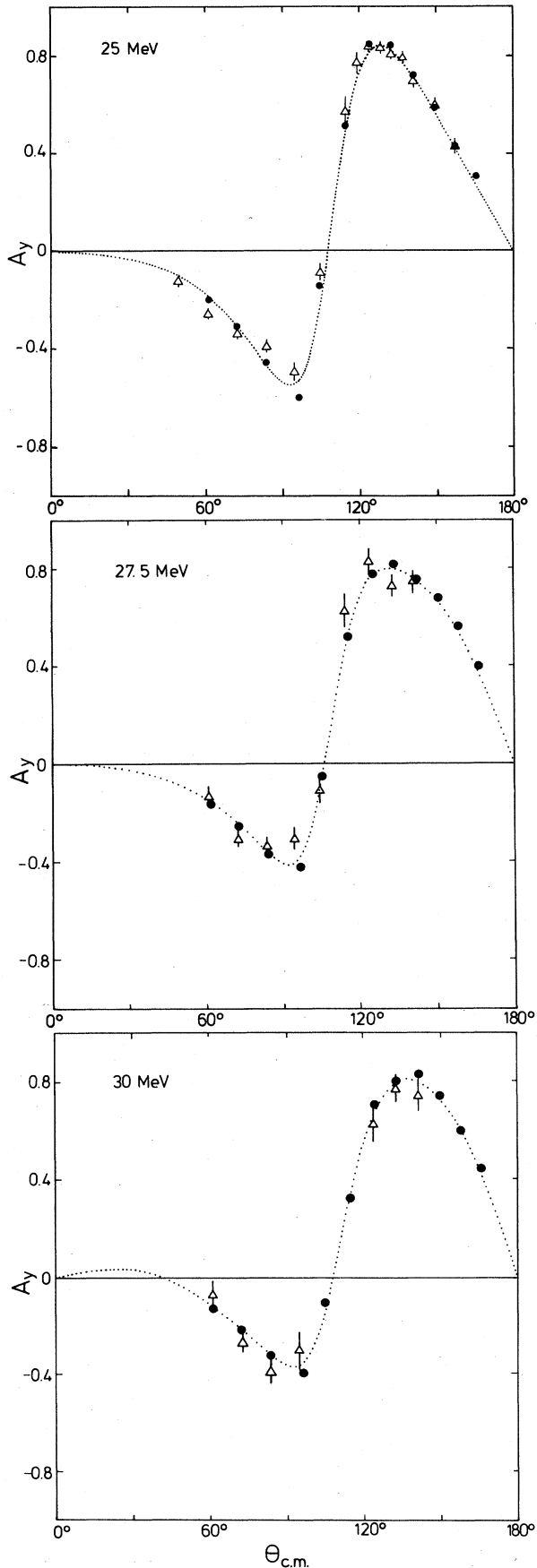


FIG. 7. \bar{n} - ${}^4\text{He}$ analyzing power distributions above inelastic threshold. Our results (full circles) are compared to the data of Ref. 25 at 25.7, 27.3, and 30.3 MeV (triangles). The dotted lines show the results of our phase-shift analyses. The statistical error of the new data in this energy range is smaller than the point size.

Above 30 MeV no accurate data on differential cross sections for the n - ${}^4\text{He}$ scattering are available. Therefore, we produced differential cross section "pseudodata" at 33, 36, 40, and 50 MeV, starting from p - ${}^4\text{He}$ phase shifts and applying Coulomb corrections as already described. The results are used as input in the phase shift analyses at these energies. To get an estimate on the reliability of this procedure the calculation was performed using various methods of Coulomb corrections as discussed extensively in Sec. III. It turned out that all methods agreed well within a few percent.

At the lower energies the Coulomb effects should be more important. Therefore, we checked the applied method at 17 MeV. In Fig. 9 the differential cross section data of Drog³¹ are compared to the results of n - ${}^4\text{He}$ phase shift analyses of Broste *et al.*²⁵ and of this work, as well as to the predictions from Coulomb corrections applied to the p - ${}^4\text{He}$ phase shifts of Schwandt *et al.*²¹ It can be seen that there is good agreement between the data and the charge symmetric prediction even at this low energy.

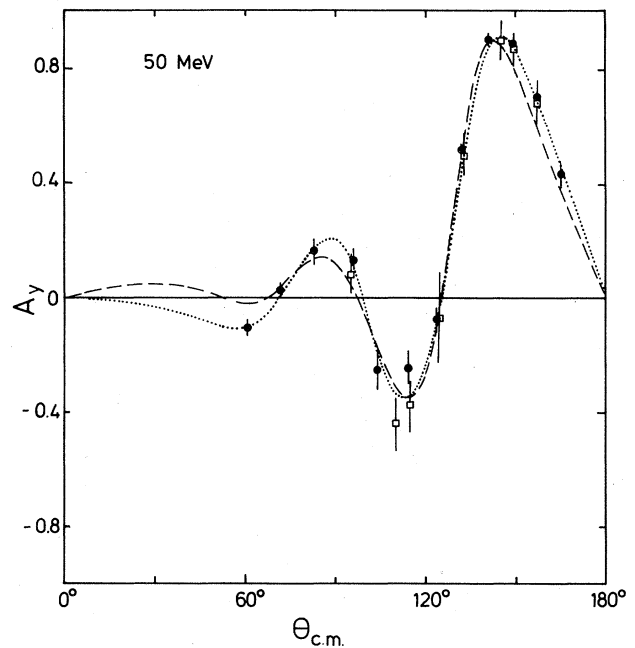


FIG. 8. \bar{n} - ${}^4\text{He}$ analyzing power at 50 MeV. Our data (full circles) are shown together with the recent results of Ref. 2 at 50.4 MeV (open squares); Coulomb correction prediction, calculated from phase shifts of Ref. 11 (dashed line); and the result of a phase-shift analysis using all new A_y data and "pseudodata" for $d\sigma/d\Omega$ (see Sec. V) (dotted line).

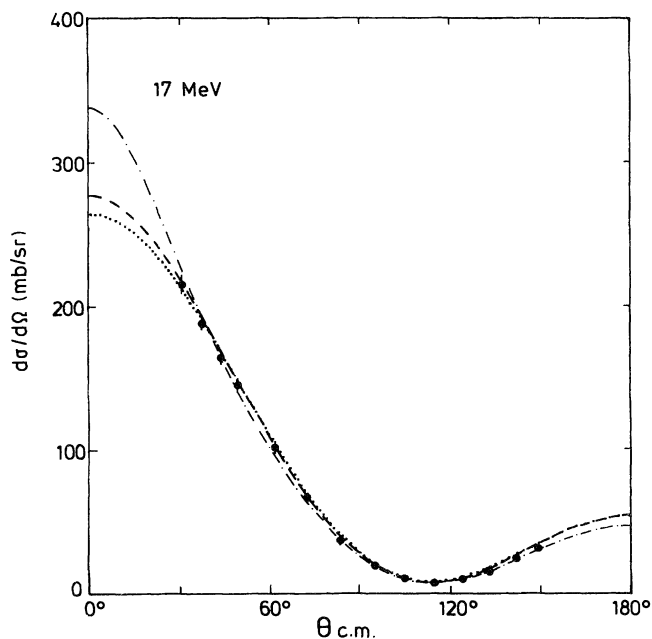


FIG. 9. Differential cross section of the elastic $n\text{-}^4\text{He}$ scattering at 17 MeV. Full circles, data of Ref. 31 at 17.6 MeV; dashed-dotted line, $n\text{-}^4\text{He}$ phase shifts from Ref. 25 at 17.7 MeV; dashed line, $n\text{-}^4\text{He}$ predictions from Coulomb corrections applied to $p\text{-}^4\text{He}$ phase shifts; and dotted line, result of the $n\text{-}^4\text{He}$ phase-shift analysis of this work.

In the phase shift analyses above 30 MeV the pseudodata were used with a low weight corresponding to an uncertainty of 20%. This produces flat minima in the search procedures with a choice of solutions which do not differ much in χ^2 and thus the analysis could be influenced strongly by single data points which might be erroneous. We tried to find a set of solutions with a reasonably smooth behavior in energy to parametrize our data. (One should be very careful, however, interpreting these phase shifts in terms of resonances.)

Figure 10 shows that at 33 and 36 MeV the phase shifts indeed reproduce both our data for A_y and the pseudodata for $d\sigma/d\Omega$ very satisfactorily. The resulting phase shifts δ (in degrees) and inelasticity parameters η are listed in Table III.

We used interpolations to these phase shifts to calculate the $n\text{-}^4\text{He}$ analyzing power in the energy range from 25 to 50 MeV in 1 MeV steps. The results are shown in Fig. 11 as a contour plot. The angular range $0^\circ\text{--}60^\circ$ is not plotted because the A_y values at the forward angles are very small and the results depend strongly on the inclusion of higher partial waves in the phase shift analyses. The A_y values which can be taken out of this contour plot are in very good agreement with our experimental data. So, we think that for the application of $n\text{-}^4\text{He}$ scattering, e.g., in neutron polarimeters for this energy range, this representation of our data may be useful.

TABLE III. $n\text{-}^4\text{He}$ phase shifts δ and inelasticity parameters η from the present single-energy analyses.

E_n (MeV)	$S_{1/2}$	$P_{3/2}$	$P_{1/2}$	$D_{5/2}$	$D_{3/2}$	$F_{7/2}$	$F_{5/2}$	$G_{9/2}$	$G_{7/2}$
15	93.87 1.00	104.18 1.00	63.71 1.00	5.07 1.00	2.22 1.00				
17	92.00 1.00	101.01 1.00	61.00 1.00	5.62 1.00	2.66 1.00				
19	89.00 1.00	100.43 1.00	59.99 1.00	9.52 1.00	6.65 1.00	0.88 1.00	0.70 1.00		
25	85.93 0.98	85.45 0.87	49.84 0.94	10.23 0.93	5.04 0.74	5.13 1.00	3.25 1.00	-0.66 1.00	0.47 0.97
27.5	83.98 0.94	83.19 0.88	45.59 0.91	12.51 0.86	5.69 0.72	6.06 1.00	4.17 1.00	-0.20 0.99	0.39 0.96
30	79.12 0.94	83.76 0.88	43.32 0.68	13.59 0.84	7.35 0.66	4.79 1.00	4.92 0.92	3.20 0.99	1.47 1.00
33	77.91 0.95	79.09 0.94	41.25 0.88	16.68 0.77	6.33 0.70	7.28 0.84	5.70 0.95	1.12 1.00	0.73 0.96
36	74.30 0.94	77.59 0.89	47.61 0.94	20.41 0.83	9.90 0.68	9.81 0.88	8.95 0.90	0.85 1.00	0.17 0.98
40	73.83 0.83	70.98 0.77	44.92 0.92	19.19 0.81	11.42 0.65	9.96 0.84	9.54 0.90	-0.11 0.99	0.14 0.97
50	70.00 0.59	63.18 0.72	30.10 0.90	19.78 0.67	15.29 0.70	15.55 0.79	8.43 0.93	3.07 0.98	0.00 1.00

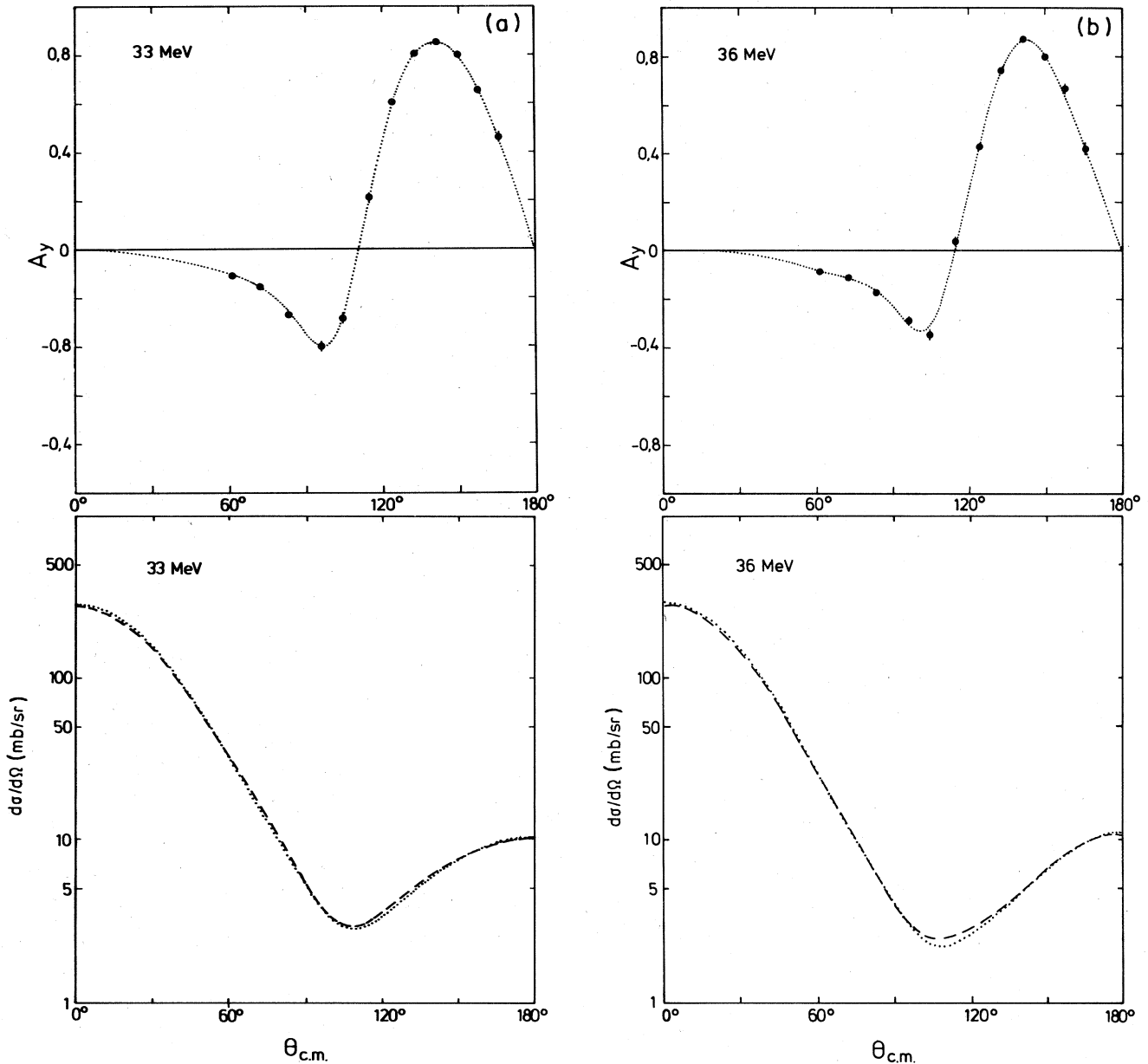


FIG. 10. Analyzing power and differential cross section at 33 and 36 MeV. Data points, this work; dashed line, Coulomb correction prediction using p - ${}^4\text{He}$ phase shifts of Ref. 10; and dotted line, result of the new n - ${}^4\text{He}$ phase-shift analysis.

VI. CONCLUSION

Angular distributions of the spin dependent asymmetry in elastic n - ${}^4\text{He}$ scattering have been measured at ten neutron energies between 15 and 50 MeV. These asymmetries have been converted to analyzing powers by normalizing in the region of the backward angle maximum of $A_y(\theta)$ as determined by (i) previous n - ${}^4\text{He}$ measurements for $E_n < 19$ MeV, (ii) p - ${}^4\text{He}$ values for $E_n = 19$ –30 MeV, and (iii) charge-symmetric n - ${}^4\text{He}$ predictions based on p - ${}^4\text{He}$ phase shifts for $E_n > 30$ MeV. These procedures seem reasonable because both the magnitude and the shape of the backward maximum of $A_y(\theta)$ are virtually identical

for p - ${}^4\text{He}$ and n - ${}^4\text{He}$ scattering over the entire 15–50 MeV range. Compared to previous n - ${}^4\text{He}$ measurements, the present data display significantly improved statistical accuracy. Scanning the energy dependence of the present data reveals a similar slight anomaly in the shape at backward angles as in p - ${}^4\text{He}$ scattering near 30 MeV.^{9,24} In the neutron case it occurs near 28 MeV, roughly compatible with the energy shift introduced by Hoop and Barschall.¹⁴

Having measured the vector polarization of the deuteron beam by d - ${}^{12}\text{C}$ elastic scattering, the vector polarization transfer coefficients, $K_y'(E_n, 0^\circ)$, have been determined for the ${}^2\text{H}(\vec{d}, \vec{n})X$ reactions at $E_d = 50$ MeV. The values obtained are in reasonable agreement with the pre-

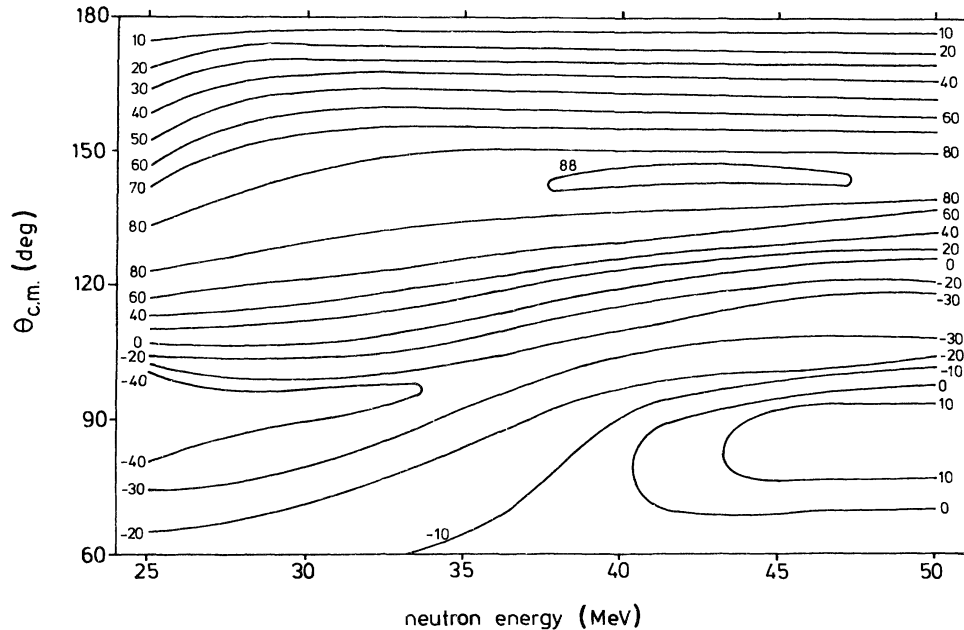


FIG. 11. Contour plot of the analyzing power of the elastic $n\text{-}^4\text{He}$ scattering in the energy range from 25 to 50 MeV, calculated from a set of phase shifts with smooth behavior in energy. A_y (in percent) is plotted in the angular range $60^\circ\text{--}180^\circ$ c.m. only. The (very small) values of A_y at forward angles depend strongly on the inclusion of higher partial waves in the phase-shift analyses.

dictions of the simple stripping model.

The validity of the charge symmetric $n\text{-}^4\text{He}$ calculations which start from $p\text{-}^4\text{He}$ phase shifts has been studied in the present work. In the 30–50 MeV region substantial differences appear between the $N\text{-}^4\text{He}$ analyzing powers in the $50^\circ < \theta_{\text{c.m.}} < 120^\circ$ range, and these differences are fairly well reproduced by the Coulomb correction calculations. It must be stressed that the charge symmetric predictions require $p\text{-}^4\text{He}$ phase shifts that exhibit a smooth energy dependence.

This is not the case with the available phase shifts near 50 MeV. The discrepancies noted between the predicted and measured neutron analyzing power distributions at this energy must, for the moment, be attributed to the uncertainties in the $p\text{-}^4\text{He}$ phases. Over the energy range studied no evidence is seen for nuclear charge symmetry breaking effects. It will be very difficult to find such effects until polarized neutron beams of at least an order of magnitude larger intensity are available.

In the $n\text{-}^4\text{He}$ phase-shift analysis presented above, for $E_n > 30$ MeV the measured analyzing powers had to be supplemented with differential cross section pseudodata obtained with the charge symmetric predictions. Al-

though the reliability of these predictions was tested at 17 MeV, less weight was given to these pseudodata in the phase-shift analysis. Consequently, the minima found in the search procedure were rather flat. Difficulty was encountered in obtaining smooth energy dependence in several phase shifts near 33 MeV. However, already in the $p\text{-}^4\text{He}$ analysis, which works on a much richer data base, multiple solutions appear at higher energies. Thus it remains that for both $p\text{-}^4\text{He}$ and $n\text{-}^4\text{He}$ scattering more precise data and possibly even more complex experiments like spin rotation measurements are necessary to improve our understanding of the $N\text{-}^4\text{He}$ interaction in this energy range.

ACKNOWLEDGMENTS

The authors are indebted to Dr. V. Bechtold, Dr. L. Friedrich, Dr. H. Schweickert, and the cyclotron team for providing the polarized deuteron beam. The valuable assistance of B. Haesner, M. Oexner, and P. Schwarz in the preparation and duration of the experiment is gratefully acknowledged.

*Permanent address: Cyclotron Institute, Texas A&M University, College Station, TX 77843.

¹P. W. Lisowski, R. L. Walter, G. G. Ohlsen, and R. A. Harkopf, *Phys. Rev. Lett.* **37**, 809 (1976).

²R. L. York, J. C. Hiebert, H. L. Woolverton, and L. C. Northcliffe, *Phys. Rev. C* **27**, 46 (1983).

³H. O. Klages, H. Dobiasch, P. Doll, H. Krupp, M. Oexner, P.

Plischke, B. Zeitnitz, F. P. Brady, and J. C. Hiebert, *Nucl. Instrum. Methods* **219**, 269 (1984).

⁴B. Haesner, Ph.D. thesis, University Karlsruhe, 1982, Kernforschungszentrum Karlsruhe Report KfK 3395, 1982.

⁵H. Krupp, diploma thesis, University Karlsruhe, 1983.

⁶T. G. Miller, F. P. Gibson, and G. W. Morrison, *Nucl. Instrum. Methods* **80**, 325 (1970).

- ⁷R. L. York, Ph.D. thesis, Texas A&M University, 1979.
- ⁸J. E. Bond and F. W. K. Firk, Nucl. Phys. **A287**, 317 (1977).
- ⁹A. D. Bacher, G. R. Plattner, H. E. Conzett, D. J. Clark, H. Grunder, and W. F. Tivol, Phys. Rev. C **5**, 1147 (1972).
- ¹⁰A. Houdayer, N. E. Davidson, S. A. Elbakr, A. M. Sourkes, W. T. H. van Oers, and A. D. Bacher, Phys. Rev. C **18**, 1985 (1978).
- ¹¹T. Saito, Nucl. Phys. **A331**, 477 (1979).
- ¹²G. Mairle, K. T. Knöpfle, H. Riedesel, G. J. Wagner, V. Bechtold, and L. Friedrich, Nucl. Phys. **A339**, 61 (1980).
- ¹³J. E. Simmons, W. B. Broste, G. P. Lawrence, J. L. McKibben, and G. G. Ohlson, Phys. Rev. Lett. **27**, 113 (1971).
- ¹⁴B. Hoop and H. H. Barschall, Nucl. Phys. **83**, 65 (1966).
- ¹⁵D. G. Dodder, G. M. Hale, N. Jarmie, J. H. Jett, P. W. Keaton, Jr., R. A. Nisley, and K. Witte, Phys. Rev. C **15**, 518 (1977).
- ¹⁶J. Fröhlich, L. Streit, H. Zankel, and H. Zingl, J. Phys. G **6**, 841 (1980); J. Fröhlich and H. Zankel Phys. Lett. **82B**, 173 (1979).
- ¹⁷M. I. Haftel and H. Zankel, Phys. Rev. C **24**, 1322 (1981); H. Zankel and G. M. Hale, *ibid.* **24**, 1384 (1981).
- ¹⁸J. Fröhlich, H. G. Schlaile, L. Streit, and H. Zingl, Z. Phys. A **302**, 89 (1981).
- ¹⁹H. Zankel, in *Polarization Phenomena in Nuclear Physics—1980 (Fifth International Symposium, Santa Fe)*, Proceedings of the Fifth International Symposium on Polarization Phenomena in Nuclear Physics, AIP Conf. Proc. No. 69, edited by G. G. Ohlson, R. E. Brown, N. Jarmie, W. W. McNaughton, and G. M. Hale (AIP, New York, 1981), p. 1413; J. Fröhlich, H. Kriesche, L. Streit and H. Zankel, Nucl. Phys. **A384**, 97 (1982).
- ²⁰H. Kriesche and H. Zankel, J. Phys. G **6**, 853 (1980).
- ²¹P. Schwandt, T. B. Clegg, and W. Haeberli, Nucl. Phys. **A163**, 432 (1971).
- ²²K. Imai, K. Hatanaki, H. Shimizu, N. Tamura, K. Egawa, N. Nisimura, T. Saito, H. Sato, and Y. Wakuta, Nucl. Phys. **A325**, 397 (1979).
- ²³J. H. Foote, O. Chamberlain, E. H. Rogers, and H. M. Steiner, Phys. Rev. **122**, 959 (1961).
- ²⁴G. R. Plattner, A. D. Bacher, and H. E. Conzett, Phys. Rev. C **5**, 1158 (1972).
- ²⁵W. B. Broste, G. S. Mutchler, J. E. Simmons, R. A. Arndt, and L. D. Roper, Phys. Rev. C **5**, 761 (1972).
- ²⁶D. C. Dodder and J. L. Gammel, Phys. Rev. **88**, 520 (1952).
- ²⁷J. L. Gammel and R. M. Thaler, Phys. Rev. **109**, 2041 (1958).
- ²⁸Th. Stambach and R. L. Walter, Nucl. Phys. **A180**, 225 (1972).
- ²⁹W. G. Weitkamp and W. Haeberli, Nucl. Phys. **83**, 46 (1966).
- ³⁰F. Ajzenberg-Selove, Nucl. Phys. **A320**, 1 (1975).
- ³¹M. Drosig, Los Alamos Scientific Laboratory Report LA-7269-MS, 1978; private communication.
- ³²B. Haesner, W. Heeringa, H. O. Klages, H. Dobiasch, G. Schmalz, P. Schwarz, J. Wilczynski, and B. Zeitnitz, Phys. Rev. C **28**, 995 (1983).
- ³³F. James and M. Roos, Comput. Phys. Commun. **10**, 343 (1975).